CF_2XCF_2X and CF_2XCF_2• Radicals (X = Cl, Br, I): Ab Initio and DFT Studies and Comparison with Experiments

Hyotcherl Ihee,[†] Jeremy Kua,[‡] William A. Goddard III,*[,‡] and Ahmed H. Zewail*[,†]

Arthur Amos Noyes Laboratory of Chemical Physics (127-72), Materials and Process Simulation Center, Beckman Institute (139−74), and Division of Chemistry and Chemical Engineering, California Institute of Technology, Pasadena, California 91125

Received: October 31, 2000; In Final Form: February 6, 2001

1,2-dihalotetrafluoroethanes (CF_2XCF_2X, X = I, Br and Cl) and halotetrafluoroethyl radicals (CF_2XCF_2•, X = I, Br, and Cl) have been studied by ab initio molecular-orbital techniques using restricted Hartree−Fock and Density functional theory (DFT-B3PW91). For the optimized HF geometries, we carried out local MP2 calculations to account for electron correlation effects. Each CF_2XCF_2X molecule and CF_2XCF_2• radical has two conformational minima (anti and gauche) and two rotational transition structures in the rotational energy surface along the C−C bond. The rotational barriers of the radicals are smaller than those of the parent molecules due to the absence of the nonbonded interaction between two halogen atoms. In contrast, the conformational energy difference between two stable rotamers (anti and gauche) of each radical is *larger* than that in the corresponding parent molecules. This stabilizing effect on the anti conformers of the radicals is rationalized in terms of hyperconjugation between the radical center and the σ^*(C−X) molecular orbital. The dissociation energies for breaking the first and second C−X bonds of CF_2XCF_2X were also calculated and compared with available experimental data. The CF_2XCF_2• radicals show dramatically different behavior compared with haloethyl radicals (CH_2XCH_2•). The CF_2XCF_2• radical has two minima and two saddle points, whereas CH_2XCH_2• radical has only one minimum and one saddle point in the rotational energy surface. In addition, the bridged structures are not stable for CF_2XCF_2• radicals in contrast with CH_2XCH_2• radicals. The origin of these differences is attributed to differences in the environment of the radical center. The calculated structures of the CF_2ICF_2• radical were used in interpreting a recent experimental observation (Cao et al. *Proc. Natl. Acad. Sci.* **1999**, *96*, 338) and are compared with quantitative results from a new experiment (Ihee et al. *Science* **2001**, *291*, 458) using the ultrafast electron diffraction technique.

1.0 Introduction

In our previous paper,[1] we reported ab initio calculations of the haloethyl radicals (CH_2XCH_2•, X = I, Br, and Cl) aimed at elucidating the origin of the stereochemical control[2−8] observed in chemical reactions involving such radicals. We found that CH_2XCH_2• has one minimum and one saddle point in the rotational energy surface along the C−C bond. In addition, we suggested that the symmetrically bridged structures[7,9,10] are highly probable and should be responsible for stereochemical control in CH_2BrCH_2• and CH_2ICH_2• radicals.

To our knowledge, there has not yet been an experimental determination of the molecular structures of CH_2XCH_2• radicals. However, the molecular structure of the fluorine substituted analogue, namely the CF_2ICF_2• radical, has recently been observed[11] and determined by[12] means of ultrafast electron diffraction techniques[13−16] developed in the Zewail laboratory. In this experiment, a CF_2ICF_2I molecule was irradiated by femtosecond laser pulses and molecular structures of transients and products were probed by picosecond electron pulses during the course of the dissociation process ($CF_2ICF_2I \rightarrow CF_2ICF_2$• + I → $CF_2{=}CF_2$ + 2I). The experimental diffraction patterns as a function of time were analyzed by incorporating geometries from the ab initio calculations reported here. We showed that the structure of the short-lived (picosecond time scale)[11,12] CF_2ICF_2• radical is consistent with the mixture of classical anti and gauche conformers found in the theory rather than the bridged structure expected for CH_2ICH_2•. Herein we provide a full account of the ab initio calculations relevant to our experimental work and a comparison with our preliminary analysis of some recent experimental results.[12]

Substitution of hydrogens with highly electronegative fluorines often causes dramatic changes in properties such as molecular structure and reactivity. For example, it is well-known that CF_3 is highly nonplanar, whereas CH_3 is planar.[17−19] The origin of this difference was explained by Goddard and Harding.[20] Another example is that 1,2-difluoroethane[21,22] (CH_2FCH_2F) strongly prefers the gauche conformer over the anti form, whereas, for CH_2ClCH_2Cl, CH_2BrCH_2Br, and CH_2ICH_2I, the anti conformer predominates over the gauche conformer (as expected from steric effects). Numerous experimental and theoretical studies have been performed to explain this effect of fluorine substitution. The comparison between CH_2XCH_2• radicals and CF_2XCF_2• radicals should provide a good platform for understanding the fluorine-substitution effect in ethyl radicals.

* To whom correspondence should be addressed. E-mail: wag@wag.caltech.edu.
[†] Arthur Amos Noyes Laboratory of Chemical Physics (127-72).
[‡] Materials and Process Simulation Center, Beckman Institute (139−74).

10.1021/jp004035x CCC: $20.00
Published on Web 03/13/2001

Along with CF_2XCF_2• radicals, 1,2-dihalotetrafluoroethanes (CF_2XCF_2X, X = I, Br and Cl) were also studied. As pointed out by Hedberg,[23] the CF_2XCF_2X system is unique because (1) it has more fluorine atoms than other heavier halogen atoms and (2) both steric and gauche effects are expected to play a role in determining the relative stability of the anti and gauche conformers. Despite the considerable number of experiments,[23−30] ab initio calculations of these molecules are quite sparse, especially for the molecules containing iodine atoms. In this work, we report studies of the structures, conformations, and dissociation energies for 1,2-dihalotetrafluoroethanes and their radicals.

2.0 Calculations

2.1 Methods. All calculations were performed using the Jaguar 3.5 program,[31,32] which utilizes pseudospectral algorithms. The C and F atoms were described using the 6-31G* basis set. The I, Br, and Cl atoms were described using the LAV3P relativistic effective core potential (RECP)[33] and basis set for the geometry scans of the rotational energy surface around the C−C bond. The LAV3P basis set consists of 3s3p valence primitive Gaussian functions contracted to 3s2p. The RECP was based on atomic calculations including relativistic effects. In addition, the stationary points were optimized with an additional basis set at the DFT-B3PW91 level.

- LAV3P(d): similar to LAV3P with an additional d-polarization function added for I, Br, and Cl atoms.[34]
- MSV: an all electron basis set equivalent to 4-31G[35]
- MSV(d): an all electron basis set equivalent to 4-31G*[35]

The DFT method (B3PW91) employs a combination of exchange terms: exact HF, the Becke 1988 nonlocal gradient correction,[36] and the original Slater local exchange functional.[37] In addition, it uses the Perdew−Wang 1991 local correlation functional and the GGA-II nonlocal correlation functional.[38]

We did not include spin−orbit coupling. This has negligible effect on the molecular radicals because the states are orbitally nondegenerate. For the dissociated halo radicals, the calculated bond energies should be decreased by $\sim(^1/_3)E(^2P_{1/2} - {}^2P_{3/2})$. This is significant only for iodine where the adiadatic bond energy would be ~8 kcal/mol lower.

2.2 Procedure. For each system, the geometry was optimized with both Hartree−Fock (HF) and density functional theory (DFT). For the optimized HF geometries, we carried out local MP2 calculations[39,40] to account for electron correlation effects, denoted LMP2//HF. All calculations were restricted to proper spin states (singlet for CF_2XCF_2X and doublet for CF_2XCF_2•).

The total energies of each molecule and radical (CF_2XCF_2X, CF_2XCF_2•, CH_2XCH_2X, CH_2XCH_2• for X = Cl, Br and I) calculated at various levels of theory and basis sets are given in the Supporting Information. The complete lists of optimized structural parameters are also provided in the Supporting Information. Selected structural parameters of the stable CF_2XCF_2X molecules are collected in Table 1 and compared with the available experimental data. In addition, selected structural parameters of the anti CF_2XCF_2• radicals are listed in Table 2 with recent experimental values[12] from ultrafast electron diffraction. For the minima and transition states, we calculated the vibrational frequencies at the HF and B3PW91 levels of theory. These frequencies were then used to obtain the zero point energy. All minima were found to have all real frequencies and all transition states were found to have only one imaginary frequency. The vibrational frequencies and mode assignments are included in the Supporting Information. The relative energies and dissociationenergies were corrected for the zero point energy using a scaling factor of 0.94 for HF and 0.97 for DFT methods.[41,42] Where the zero point energies are not calculated, values obtained with the same level of theory were used. For example, for energies with LMP2//HF (LAV3P), we used the zero point corrections from HF (LAV3P) calculations. Table 3 lists the conformational energy differences and rotational barriers.

3.0 Results and Discussion

3.1 CF_2XCF_2X (X = I, Br, and Cl). The CF_2XCF_2X molecule has two conformational minima, A (anti) and G (gauche), on the rotational energy surface. The two rotational transition structures connecting A and G are denoted as T1 (G ↔ G) and T2 (G ↔ A). The structures are schematically represented in Figure 1, with the rotational energy surfaces calculated at the LMP2//HF level. The anti conformer exhibits C_{2h} symmetry, whereas the gauche conformer has C_2 symmetry. The structures of these molecules have been well studied by gas-phase electron diffraction.[23,24,30] The experimental values from the literature[23,24,30] are also listed in Table 1 for comparison.

3.1.1 Geometries. The experimental structural parameters were obtained assuming that the anti and gauche conformers have identical geometry except for the ICCI dihedral angle.[23,24] At the HF level of theory with the LAV3P(d) basis set, we find the following for CF_2ICF_2I:

CC bond distances of 1.532 Å for A and 1.540 Å for G (1.534 ± 0.013 experiment);

CF bond distances of 1.320 Å for A and 1.323 Å for G (1.328 ± 0.003 experiment);

CI bond distances of 2.159 Å for A and 2.147 Å for G (2.136 ± 0.007 experiment);

CCF bond angles of 109.0° for A and 107.6° for G (109.4° ± 1.0° experiment);

CCI bond angles of 111.9° for A and 114.8° for G (111.6° ± 1.0° experiment);

FCF bond angles of 108.7° for A and 107.9° for G (107.8° ± 1.0° experiment).

Generally, the geometries optimized at the HF and B3PW91 levels are very close to the experimental structures. Compared with the HF structures, the DFT (B3PW91) structures differ by less than 0.02 Å for the CC and CF bond distances, less than 0.04 Å for the CX bond distances, less than 1° for the CCF and FCF bond angles, and less than 2° for the CCX bond angles (see Table 1). A closer examination reveals that the B3PW91 method gives longer CC, CF, and CX bond distances than those of the HF method, and within the B3PW91 method, the LAV3P(d) basis set provides the closer values to the available experimental values than the LAV3P basis set. Compared with the available experimental values, the B3PW91(LAV3P(d)) optimized values have longer CC, CF, and CX bond distances. For the CX bond distance, the HF (LAV3P(d)) gives better agreement with the experiment than the B3PW91 method. For the CC and CF distances, the B3PW91 method gives better agreement with the experiment than the HF method. As mentioned previously, the experimental values were obtained with a simplifying assumption that the anti and gauche conformers have the exact same structural parameters except for the XCCX dihedral angle. Our calculations suggest that the C−C and C−F distances of the anti conformers are smaller and C−X distances are longer than those of the gauche conformers.

On the basis of electron diffraction studies, Hedberg and coworkers reported that the internuclear distances between halogen atoms, which are gauche to each other, are smaller than the

TABLE 1: Selected Structural Parameters of CF_2XCF_2X (X = I, Br, Cl)[c]

X = I	expt[a,n]	HF (LAV3P)	**HF (LAV3P(d))**	B3PW91 (LAV3P)	B3PW91 (LAV3P(d))	B3PW91 (MSV)	B3PW91 (MSV(d))
				A			
C−C	1.534 (13)	1.531	**1.532**	1.545	1.547	1.529	1.542
C−F	1.328 (3)	1.319	**1.320**	1.333	1.335	1.394	1.336
C−X	2.136 (7)	2.169	**2.159**	2.207	2.187	2.167	2.198
CCF	109.4 (10)	109.0	**109.0**	109.7	109.6	108.4	109.5
CCX	111.6 (10)	112.0	**111.9**	110.4	110.5	113.9	110.6
FCF	107.8 (10)	107.8	**108.7**	109.4	109.3	107.5	109.3
XCCX	180 (fixed)	180.0	**180.0**	180.0	180.0	180.0	180.0
F...F	2.734 (13)	2.708	**2.712**	2.746	2.749	2.784	2.743
X...X	5.054 (7)	5.112	**5.092**	5.161	5.129	5.146	5.146
F...X	3.256 (9)	3.274	**3.267**	3.304	3.293	3.319	3.295
				G			
C−C	1.534 (13)	1.537	**1.540**	1.555	1.556	1.538	1.552
C−F	1.328 (3)	1.321	**1.323**	1.337	1.339	1.395	1.340
C−X	2.136 (7)	2.159	**2.147**	2.193	2.173	2.167	2.186
CCF	109.4 (10)	107.4	**107.6**	108.0	108.2	107.7	107.9
CCX	111.6 (10)	115.0	**114.8**	113.3	113.0	115.6	113.7
FCF	107.8 (10)	108.0	**107.9**	108.5	108.4	107.0	108.5
XCCX	70 (3)	67.3	**67.8**	67.8	68.2	63.8	60.5
F...F	2.62 (3)	2.535	**2.540**	2.744	2.594	2.640	2.645
X...X	3.87 (5)	4.002	**3.987**	3.985	3.952	3.988	3.873
F...X	3.17 (3)	3.307	**3.293**	3.311	3.284	3.377	3.385
X = Br				A			
C−C	1.548 (13)	1.531	**1.536**	1.547	1.552	1.529	1.544
C−F	1.332 (3)	1.312	**1.316**	1.329	1.333	1.387	1.335
C−X	1.922 (5)	1.976	**1.944**	2.011	1.972	1.963	1.948
CCF	109.9 (4)	109.5	**109.2**	110.0	109.6	109.0	109.5
CCX	110.5 (5)	110.7	**111.1**	109.6	109.0	112.5	110.0
FCF	108.4 (8)	109.3	**108.9**	109.8	109.4	108.0	109.3
XCCX	180 (fixed)	180.0	**180.0**	180.0	180.0	180.0	180.0
F...F	2.774 (12)	2.707	**2.712**	2.746	2.750	2.784	2.744
X...X	4.631 (8)	4.714	**4.666**	4.749	4.708	4.727	4.655
F...X	3.123 (7)	3.123	**3.108**	3.159	3.139	3.164	3.111
				G			
C−C	1.548 (13)	1.536	**1.540**	1.553	1.556	1.534	1.549
C−F	1.332 (3)	1.315	**1.319**	1.333	1.336	1.388	1.338
C−X	1.922 (5)	1.966	**1.935**	1.997	1.960	1.958	1.936
CCF	109.9 (4)	108.0	**107.9**	108.6	108.3	108.4	108.4
CCX	110.5 (5)	113.4	**113.6**	112.1	112.3	113.7	111.8
FCF	108.4 (8)	108.6	**108.2**	108.9	108.6	107.7	108.6
XCCX	67 (3)	66.0	**65.9**	66.6	66.1	65.4	63.6
F...F	2.71 (3)	2.568	**2.569**	2.620	2.622	2.660	2.644
X...X	3.52 (5)	3.668	**3.639**	3.668	3.628	3.662	3.539
F...X	3.06 (4)	3.147	**3.134**	3.158	3.142	3.173	3.134
X = Cl				A			
C−C	1.557 (7)	1.533	**1.538**	1.549	1.555	1.533	1.551
C−F	1.330 (2)	1.310	**1.316**	1.329	1.335	1.379	1.336
C−X	1.747 (3)	1.783	**1.743**	1.817	1.768	1.846	1.770
CCF	108.9 (3)	109.4	**108.9**	109.8	109.2	109.7	109.2
CCX	110.7 (4)	110.3	**111.0**	109.5	110.4	110.7	110.3
FCF	108.7 (3)	109.5	**108.9**	109.8	109.2	108.7	109.1
XCCX	180 (fixed)	180.0	**180.0**	180.0	180.0	180.0	180.0
F...F	2.745 (7)	2.703	**2.708**	2.743	2.747	2.792	2.745
X...X	4.305 (9)	4.342	**4.286**	4.400	4.330	4.470	4.330
F...X	2.994 (6)	2.991	**2.973**	3.029	3.006	3.072	3.003
				G			
C−C	1.557 (7)	1.536	**1.540**	1.552	1.557	1.537	1.553
C−F	1.330 (2)	1.313	**1.318**	1.332	1.337	1.382	1.340
C−X	1.747 (3)	1.776	**1.739**	1.807	1.762	1.838	1.763
CCF	108.9 (3)	108.2	**107.9**	108.7	108.3	109.2	108.4
CCX	110.7 (4)	112.8	**113.1**	111.6	112.1	111.7	111.8
FCF	108.7 (3)	108.9	**108.4**	109.1	108.6	108.2	108.6
XCCX	62.5 (13)	64.6	**64.0**	65.7	64.7	65.4	63.7
F...F	2.695 (13)	2.588	**2.587**	2.640	2.634	2.699	2.645
X...X	3.273 (20)	3.396	**3.361**	3.411	3.370	3.432	3.343
F...X	2.986 (17)	3.017	**3.007**	3.028	3.018	3.057	3.019

[a] r_e values for X = I and Br estimated from electron diffraction data[23] [b] r_e values for X = Cl estimated from electron diffraction data[30] [c] The experimental data and the calculated values at various levels of theory (HF and B3PW91) and basis set (LAV3P, LAV3P(d), MSV, and MSV(d)) are presented for comparison. The prefix A- and G-mean anti- and gauche-, respectively. For F...F, X...X, and F...X, only the shortest pairs are listed. We recommend the HF (LAV3P(d)) values for structures

TABLE 2: Selected Structural Parameters of the Anti $CF_2XCF'_2$• (X = I, Br, Cl) Radicals[b]

	experiment[a]	HF (LAV3P)	HF (LAV3P(d))	B3PW91 (LAV3P)	B3PW91 (LAV3P(d))	B3PW91 (MSV)	B3PW91 (MSV(d))
X = I							
r(C═C)	1.478 ± 0.049	1.502	**1.503**	1.489	1.492	1.486	1.490
r(C−F)	1.340 ± 0.037	1.320	**1.322**	1.334	1.336	1.394	1.337
r(C−X)	2.153 ± 0.013	2.180	**2.164**	2.266	2.233	2.193	2.229
r(C−F′)	1.277 ± 0.027	1.304	**1.304**	1.315	1.316	1.363	1.318
∠CCX	115.0 ± 3.1	113.0	**112.7**	111.3	111.5	115.2	109.8
∠CCF	108.6 ± 6.0	108.5	**108.6**	110.1	109.9	108.4	110.2
∠FCF/2	54.0 ± 5.6	54.4	**54.4**	55.0	54.9	54.2	54.9
∠CCF′	117.9 ± 3.1	114.0	**114.0**	116.1	115.9	116.1	115.3
∠F′CF′/2	59.9 ± 3.9	55.9	**55.9**	56.4	56.4	56.0	56.4
X = Br							
r(C═C)		1.502	**1.505**	1.493	1.500	1.486	1.497
r(C−F)		1.315	**1.319**	1.331	1.336	1.388	1.337
r(C−X)		1.989	**1.952**	2.063	2.006	2.001	1.982
r(C−F′)		1.303	**1.304**	1.316	1.317	1.361	1.319
∠CCX	Not available	111.9	**112.1**	111.0	111.6	113.9	111.3
∠CCF		109.1	**108.8**	110.3	109.7	109.0	109.6
∠FCF/2		54.7	**54.4**	55.1	54.9	54.4	54.8
∠CCF′		113.9	**113.9**	115.8	115.5	116.1	115.2
∠F′CF′/2		54.4	**56.0**	56.4	56.4	56.1	56.4
X = Cl							
r(C═C)		1.504	**1.507**	1.501	1.508	1.486	1.504
r(C−F)		1.313	**1.319**	1.331	1.338	1.382	1.339
r(C−X)		1.797	**1.752**	1.856	1.793	1.885	1.795
r(C−F′)		1.303	**1.304**	1.318	1.319	1.360	1.320
∠CCX	Not available	111.6	**112.2**	111.2	112.3	111.9	112.2
∠CCF		109.3	**108.6**	110.0	109.1	110.0	109.1
∠FCF/2		54.7	**54.4**	53.9	54.7	54.6	54.7
∠CCF′		113.6	**113.6**	115.1	114.9	116.0	114.9
∠F′CF′/2		56.0	**55.9**	56.4	56.2	56.3	56.3

[a] r_e values from recent ultrafast electron diffraction data.[12] [b] The calculated values at various levels of theory (HF and B3PW91) and basis set (LAV3P, LAV3P(d), MSV, and MSV(d)) are presented. Values from preliminary analysis of recent ultrafast electron diffraction experiment are also given for comparison. We recommend the HF (LAV3P(d)) values for structures.

corresponding van der Waals distances by 0.2 to 0.6 Å. They suggested that the small root-mean square amplitudes of the torsional motion can be explained by the minimization of van der Waals repulsion.[23] The C−C distances in the rotational transition structures are even longer than those of anti and gauche structures by 0.03 Å. The elongation of C−C bonds in gauche conformers and the transition structures (provided in the Supporting Information) can be readily explained by the same argument.

3.1.2 Energies. The conformational energy differences and rotational barriers are listed in Table 3. The correction for the thermal energies (0 to 300 K) are less than 0.1 kcal/mol and are not included. The energy differences between the anti and gauche conformers of CF_2XCF_2X were investigated by infrared spectroscopy[25−29] and gas-phase electron diffraction.[23,24] For all three molecules, anti conformers were found to be more stable than gauche conformers, in agreement with our calculations.

Serboli and Minasso[29] measured the infrared spectrum of CF_2ICF_2I at various temperatures and phases, and deduced $\Delta E_{A\rightarrow G} = 1.835 \pm 0.100$ kcal/mol. Using the same approach, Kagarise and Daasch[27,28] reported $\Delta E_{A\rightarrow G} = 0.925 \pm 0.050$ kcal/mol for CF_2BrCF_2Br and 0.5 ± 0.2 kcal/mol for CF_2ClCF_2Cl. Hedberg and co-workers[23,30] obtained a slightly lower value of 1.22 ± 0.36 kcal/mol for CF_2ICF_2I, 0.86 ± 0.26 kcal/mol for CF_2BrCF_2Br, and 0.45 ± 0.11 kcal/mol for CF_2ClCF_2Cl by measuring mole fractions of gauche conformers at various temperatures. Iwasaki[24] also used the gas-phase electron diffraction technique and obtained 0.44 ± 0.11 kcal/mol for CF_2ClCF_2Cl.

The conformational energy differences obtained using the single-point energies calculated at LMP2//HF (LAV3P(d)) level of theory are in good agreement with the experimentally obtained values for all three molecules. Thus, at the LMP2// HF level, we find

$\Delta E_{A\rightarrow G} = 1.90$ for X = I (experiment 1.835 ± 0.1 and 1.22 ± 0.36)

$\Delta E_{A\rightarrow G} = 1.05$ for X = Br (experiment 0.925 ± 0.05 and 0.81 ± 0.26)

$\Delta E_{A\rightarrow G} = 0.44$ for X = Cl (experiment 0.5 ± 0.2 and 0.44 ± 0.11)

In general, the inclusion of a d function reduces the energy differences between the conformers giving closer values to the experiment. Both experiment and ab initio calculations show that the conformational energy difference increases on the order of Cl, Br, and I. This trend is consistent with the idea that the main source for the different stabilities of anti and gauche conformers is steric. Indeed, the X...X distance for G at the HF level of theory is 3.396 Å for Cl, 3.668 Å for Br, and 4.002 Å for I, all less than standard van der Waals parameters 3.92 Å for Cl, 4.19 Å for Br, and 4.50 Å for I (values from the DREIDING force field[43]). The X...X distance calculated with the B3PW91 method is also smaller than the van der Waals parameters. The Supporting Information provides graphs showing such correlations in the conformational energy differences.[44] The barriers for the internal rotation also follow the same trend; the bigger the halogen atom, the higher the barrier.

Since the discovery of rotational barriers and conformational energies, there have been numerous discussions[21,44−61] regarding their origin. Although this is not the focus of this paper, a few

TABLE 3: Relative Energies Calculated at Various Levels of Theory (HF and B3PW91) and Basis Sets (LAV3P, LAV3P(d), MSV, and MSV(d)) for CF_2XCF_2X and CF_2XCF_2• Radicals (X = I, Br, Cl)[g]

CF_2XCF_2X				
method	A-CF_2ICF_2I	G-CF_2ICF_2I	T1-CF_2ICF_2I	T2-CF_2ICF_2I
HF (LAV3P)	−3.59	0	10.09	4.90
HF (LAV3P(d))	−2.97	0	10.01	5.16
LMP2//HF (LAV3P)	−2.17	0	9.42	5.28
LMP2//HF (LAV3P(d))	**−1.90**	**0**	**8.96**	**4.83**
B3PW91 (LAV3P)	−3.16	0	7.41	3.36
B3PW91 (LAV3P(d))	−3.13	0	6.74	2.88
B3PW91 (MSV)	−3.70	0	7.90	3.19
B3PW91 (MSV(d))	−2.98	0	7.24	3.23
Expt[a]	−1.835 ± 0.10	0		
Expt[b]	−1.22 ± 0.36	0		
method	A-CF_2BrCF_2Br	G-CF_2BrCF_2Br	T1-CF_2BrCF_2Br	T2-CF_2BrCF_2Br
HF (LAV3P)	−2.27	0	9.17	5.37
HF (LAV3P(d))	−1.52	0	8.99	5.82
LMP2//HF (LAV3P)	−1.06	0	8.13	5.49
LMP2//HF (LAV3P(d))	**−1.05**	**0**	**7.82**	**5.12**
B3PW91 (LAV3P)	−1.62	0	7.01	4.26
B3PW91 (LAV3P(d))	−1.12	0	6.60	4.21
B3PW91 (MSV)	−1.79	0	7.28	4.15
B3PW91 (MSV(d))	−1.17	0	6.83	4.50
Expt[c]	−0.925 ± 0.05	0		
Expt[b]	−0.86 ± 0.26	0		
method	A-CF_2ClCF_2Cl	G-CF_2ClCF_2Cl	T1-CF_2ClCF_2Cl	T2-CF_2ClCF_2Cl
HF (LAV3P)	−1.24	0	8.10	5.96
HF (LAV3P(d))	−0.83	0	8.20	6.35
LMP2//HF (LAV3P)	−0.49	0	6.90	5.40
LMP2//HF (LAV3P(d))	**−0.44**	**0**	**7.28**	**5.75**
B3PW91 (LAV3P)	−0.82	0	6.22	4.39
B3PW91 (LAV3P(d))	−0.37	0	6.10	4.64
B3PW91 (MSV)	−0.91	0	6.69	4.63
B3PW91 (MSV(d))	−0.27	0	6.04	4.76
Expt[d]	−0.5 ± 0.2	0		
Expt[e]	−0.44 ± 0.11	0		
Expt[f]	−0.45 ± 0.11	0		

CF_2XCF_2• radicals					
method	A-CF_2ICF_2	G-CF_2ICF_2	T1-CF_2ICF_2	T2-CF_2ICF_2	B−CF_2ICF_2
HF (LAV3P)	−2.83	0	2.61	2.41	58.85
HF (LAV3P(d))	−2.61	0	2.58	2.52	56.65
LMP2//HF (LAV3P)	−3.55	0	2.44	1.95	34.48
LMP2//HF (LAV3P(d))	−3.33	0	2.26	1.61	31.78
B3PW91 (LAV3P)	−5.02	0	1.51	1.09	30.10
B3PW91 (LAV3P(d))	−4.62	0	1.50	1.08	27.77
B3PW91 (MSV)	−2.96	0	1.76	0.88	29.61
B3PW91 (MSV(d))	−4.76	0	1.56	1.033	27.06
method	A-CF_2BrCF_2	G-CF_2BrCF_2	T1-CF_2BrCF_2	T2-CF_2BrCF_2	B−CF_2BrCF_2
HF (LAV3P)	−2.83	0	2.47	2.56	71.30
HF (LAV3P(d))	−2.07	0	2.53	2.76	70.16
LMP2//HF (LAV3P)	−2.90	0	2.33	2.22	44.60
LMP2//HF (LAV3P(d))	−2.75	0	2.12	1.93	41.77
B3PW91 (LAV3P)	−3.94	0	1.57	1.42	39.37
B3PW91 (LAV3P(d))	−3.22	0	1.69	1.45	38.62
B3PW91 (MSV)	−2.44	0	2.04	1.35	40.89
B3PW91 (MSV(d))	−3.09	0	1.88	1.47	40.02
method	A-CF_2ClCF_2	G-CF_2ClCF_2	T1-CF_2ClCF_2	T2-CF_2ClCF_2	B−CF_2ClCF_2
HF (LAV3P)	−1.80	0	2.61	2.62	84.14
HF (LAV3P(d))	−1.53	0	2.81	2.75	25.16
LMP2//HF (LAV3P)	−2.07	0	2.55	2.29	59.29
LMP2//HF (LAV3P(d))	−1.79	0	2.45	2.05	31.26
B3PW91 (LAV3P)	−2.70	0	1.90	1.55	10.64
B3PW91 (LAV3P(d))	−2.05	0	2.23	1.63	18.16
B3PW91 (MSV)	−2.27	0	1.89	1.54	10.83
B3PW91 (MSV(d))	−1.98	0	2.19	1.64	17.34

[a] IR spectroscopy.[29] [b] Electron diffraction.[23] [c] IR spectroscopy.[28] [d] IR spectroscopy.[27] [e] Electron diffraction.[24] [f] Electron diffraction.[30] [g] The energies are given in kcal/mol. The prefixes A-, G-, T-, and B- mean anti-, gauche-, transition state, and bridged structure, respectively. For energies, we recommend the LMP2//HF (LAV3P(d)) values.

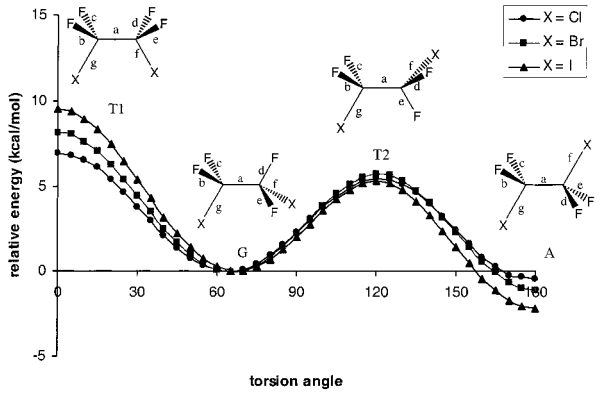

Figure 1. Rotational potential energy curves for the CF_2XCF_2X (X = I, Br, and Cl) molecules calculated at LMP2//HF (LAV3P). The torsion angle is the XCCX dihedral angle.

comments are relevant. In the force fields used for molecular dynamics, the energy is composed of additive interactions.[45] Here, the steric interactions between the nonbonded substituents are described in terms of van der Waals and electrostatic interactions. This is supplemented with a torsional term to obtain a more precise fit. The van der Waals term accounts for Pauli orthogonalization of nonbonded orbitals (repulsive) and long-range attraction (dispersion). These pair repulsions dominate the steric interaction responsible for the conformational energy difference between the anti and gauche forms of the CF_2XCF_2X molecules.[48] There have been many attempts to analyze the QM conformational energies and rotational barriers in terms of orbital interactions[21,56,62] or energy decompositions.[46,49,50] One energy decomposition[46] partitions the total HF energy into the attractive energy (total one-electron energy terms) and the repulsive energy (nuclear repulsion energy plus total two-electron energy terms). This is shown for CF_2ICF_2I in Figure 2. This figure shows that the rotational barriers are attractive-dominant, whereas the conformational energy is repulsive-dominant. For example, transforming the gauche conformer into the transition states, the change of the attractive energy is bigger than that of the repulsive energy and therefore is more responsible for the origin of the barriers (attractive-dominant). In contrast, the opposite is true for converting the gauche to the anti form (repulsive-dominant). The repulsive-dominant interaction is due to the steric effect in the force field. The energy decompositions for CF_2ICF_2•, CH_2ICH_2I, and CH_2ICH_2• are included in the Supporting Information. Comparing the rotational barriers and conformational energy differences (presented in the Supporting Information) between CF_2XCF_2X and CH_2XCH_2X shows that the barriers of CF_2XCF_2X are generally higher and the conformational energy difference is lower than those of CH_2XCH_2X.

3.2 CF_2XCF_2• Radicals (X = I, Br, and Cl). *3.2.1 Classical Asymmetric Structure.* The CF_2XCF_2 radicals can be readily observed in the photodissociation reactions of CF_2XCF_2X molecules.[11,12,63−67] As with the parent molecules, each radical has two minima, A (anti) and G (gauche), and two rotational transition states, T1 and T2, on the rotational energy surface. The structures are schematically illustrated in Figure 3 with the rotational energy surfaces calculated at the LMP2//HF level. The anti conformers have C_s symmetry, and the gauche conformers have C_1 symmetry. The geometries of these radicals have not yet been studied experimentally with the exception of the ultrafast electron diffraction study[11,12] on the CF_2ICF_2• radical.

Table 2 presents selected structural parameters of the anti CF_2XCF_2 radicals. The general trend of the structural parameters in the radicals is the same as for the parent molecules. The

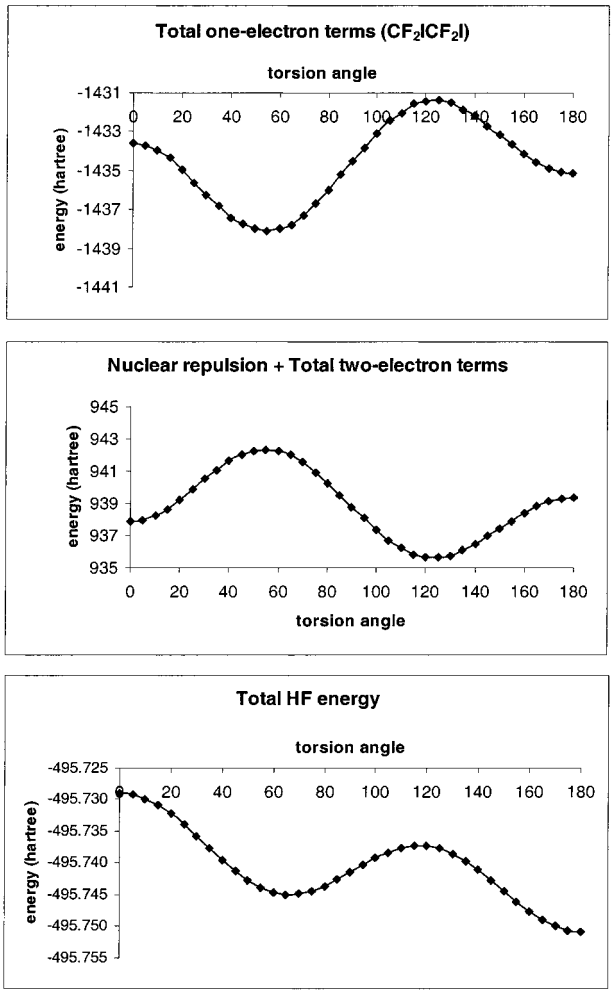

Figure 2. Energy decomposition for CF_2ICF_2I calculated at HF (LAV3P) level. Total HF energy is sum of the attractive energy (Total one-electron term) and repulsive energy (Nuclear repulsion + Total two-electron terms). See 3.1.2 for a discussion.

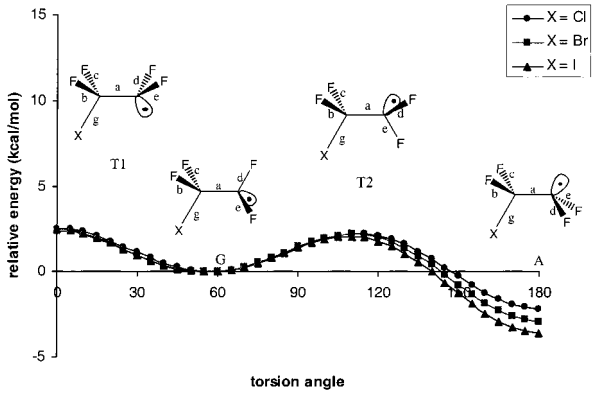

Figure 3. Rotational potential energy curves for the CF_2XCF_2 (X = I, Br, and Cl) radicals calculated at LMP2//HF (LAV3P). The torsion angle is the dihedral angle of XCC-radical center.

gauche conformers have longer C−C bonds and shorter C−X bonds than the anti conformers. The structures in the rotational transition state structures also have highly elongated C−C bonds.

The B3PW91 method generally gives longer CF, CF′, and CX bond distances than those of the HF method, and the HF (LAV3P(d)) method actually provides the closest C−I distance to the experimental value from the analysis of recent data[12] using ultrafast electron diffraction. This result is consistent with the trend observed in the parent molecules, which also show that

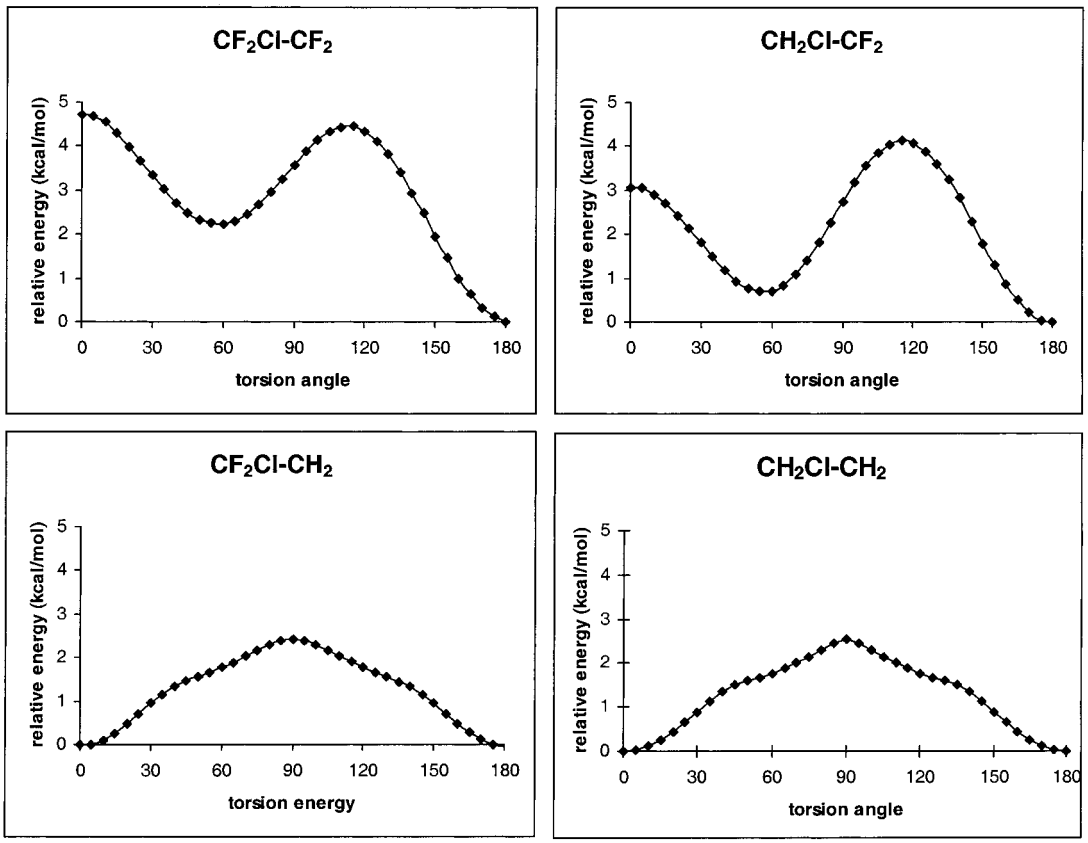

Figure 4. Rotational potential energy curves for various radicals calculated at LMP2//HF (LAV3P). The torsion angle is the dihedral angle of XCC-radical center. Note that the lower two cases correspond to equivalent isomers for $\phi = 0$ to 180° because the radical center is CH_2 which prefers to be planar.

the HF (LAV3P(d)) values are the closest values to the experiment. For the CC and CF distances, the B3PW91 methods gives better values than the HF method and this trend is also similar to that for the parent molecule (CF_2ICF_2I). The experimentally determined structural parameters of the CF_2ICF_2I and CF_2ICF_2 shows the same trend as predicted by calculations. The C−I bond distance becomes longer (∼0.02 Å) and the C−C bond distance becomes shorter (∼0.05 Å) for the CF_2-ICF_2 radical compared with the CF_2ICF_2I molecule. In addition, the CCF′ and F′CF′ angles become larger by 9° and 11°, suggesting that the radical center ($-CF'_2$) of the CF_2ICF_2 radical is relaxed after removing the I atom from the CF_2ICF_2I molecule.

Table 3 presents the relative energies for different conformations of the CF_2XCF_2 radicals. No experimental values for the radicals have been reported yet. We find that these anti conformers are more stable than the gauche conformers by 1.8 kcal/mol (at LMP2//HF (LAV3P(d))) for Cl, 2.8 kcal/mol for Br, and 3.3 kcal/mol for I; thus, the radicals follow the same trend as seen in the parent molecules but with much larger amount. The barriers also increase on the order of Cl, Br, and I, as for the parent but with much lower amount. Both T1 and T2 rotational barriers are significantly lowered compared to those of the parent molecules. The lowered rotational barriers in the radicals can be readily explained by the absence of the steric repulsion between two heavy halogen atoms (I, Br, and Cl). However, the larger conformational energy differences in the radicals cannot be explained solely by the steric effect since steric repulsion in the gauche conformer should be less severe for the radicals than the parent molecules.

The larger conformational energy differences in the radicals suggest that the anti form of the radical gains extra stability. Indeed, the anti conformer has a hyperconjugative interaction[1] between the radical center and the σ^*(C−X) MO, whereas the gauche form has hyperconjugation between the radical center and the σ^*(C−F) MO. The more electronegative atom will disfavor the hyperconjugation by raising the energy of the σ^*-(C−X) MO. To further confirm our conclusion, we compared the (B3PW91) relative energies of the CI_2FCI_2F molecule with the CI_2FCI_2 radical. For CI_2FCI_2F, the anti conformer is more stable than the gauche form by 1.41 kcal/mol mainly due to steric effects. For the radical, the relative stability is *reversed* with the gauche form more stable than the anti form by 7.43 kcal/mol. This is highly consistent with the hyperconjugation explanation because the anti form of the CI_2FCI_2 radical has hyperconjugation between the radical center and the σ^*(C−F) MO, whereas the gauche form has hyperconjugation between the radical center and the σ^*(C−I) MO.

In Table 3, the comparison of B3PW91 (LAV3P) and B3PW91 (LAV3P(d)) shows that the inclusion of a d function to the halogen atom does not change the general energetics of the conformers. The CH_2XCH_2 radicals have only one minima and one saddle point (see Figure 4), whereas the CF_2XCF_2 radicals have two minima and two saddle points on the rotational energy surface. This rather dramatic change is due to the difference in the radical center; in CH_2XCH_2 radicals, the radical center is almost planar; however, the radical center of CF_2XCF_2 is highly nonplanar due to the electronegative F atoms. The effect of fluorine substitution was systematically studied by Bernardi, et al.[19] for the fluorine substituted methyl radicals ($CH_{3-n}F_n$, $n = 0-3$). They showed that the pyramidality of the radical center increases with fluorination due to conjugative and inductive effects. The nonplanarity of the CF_2XCF_2 radicals can be explained by the same argument.

TABLE 4: Relative Energies (in kcal/mol) Calculated at Various Levels of Theory (HF and B3PW91) and Basis Sets (LAV3P and LAV3P(d)) for CH_2XCH_2• Radicals (X = I, Br, Cl)[a]

	CH_2XCH_2	
method	A-CH_2ICH_2	B-CH_2ICH_2
HF (LAV3P)	12.28 (2.246 Å)	0 (3.894 Å)
B3PW91 (LAV3P)	converged to bridge	0 (3.079 Å)
B3PW91 (LAV3P(d))	converged to bridge	0 (3.046 Å)
method	A-CH_2BrCH_2	B-CH_2BrCH_2
HF (LAV3P)	6.09 (2.062 Å)	0 (3.620 Å)
B3PW91 (LAV3P)	0.99 (2.170 Å)	0 (2.829 Å)
B3PW91 (LAV3P(d))	−1.98 (2.074 Å)	0 (2.774 Å)
method	A-CH_2ClCH_2	B-CH_2ClCH_2
HF (LAV3P)	−3.00 (1.875 Å)	0 (3.515 Å)
B3PW91 (LAV3P)	−4.63 (1.931 Å)	0 (2.660 Å)
B3PW91 (LAV3P(d))	−10.01 (1.847 Å)	0 (2.633 Å)

[a] The energies are given in kcal/mol. The prefix A- and B− mean anti and bridged structure. the values in the parentheses are the C−X bond distances.

We explored the rotational potential energy surfaces of CF_2-$ClCF_2$•, CF_2ClCH_2•, CH_2ClCF_2•, CH_2ClCH_2• radicals as shown in Figure 4. Indeed, we found that every species having a $-CH_2$• radical center has only one stable conformation (which is anti with one rotational transition structure), whereas radicals with a $-CF_2$• center have two minima and two transition states on the rotational energy surface along the C−C bond.

3.2.2 Bridged Structure. Our previous study[1] of CH_2BrCH_2 and CH_2ICH_2 radicals showed that the symmetrically bridged form is stable in the potential energy surfaces, confirming the Skell hypothesis[7,9,10] that symmetrical bridging is predominantly responsible for stereochemical control. In our previous study on the CH_2XCH_2 radicals (X = I, Br, and Cl), the LAV3P basis set was used without a d function. To test the effect of a d function, the geometries of the CH_2XCH_2 radicals were optimized with the LAV3P(d) basis set at the B3PW91 level of theory and compared with the previous values[1] in Table 4. Inclusion of a d function shortens the C−X bond distances, but not dramatically. Moreover, the anti structures get added stabilization compared with the bridged structures, and for the CH_2BrCH_2 radical, the bridged structure is less stable than the anti structure. Therefore, our previous conclusion that the bridged form of the CH_2BrCH_2 radical is more stable than the anti form should be modified; the anti form is more stable than the bridged form in the B3PW91 (LAV3P(d)) calculation. This new conclusion is consistent with a MRD-CI calculation[68] of Engels and Peyerimhoff. However, the bridged structure is still the global minimum for the CH_2ICH_2 radical.

The bridged structures were also explored in an attempt to elucidate the relative stability of the bridged CF_2XCF_2 radicals. Table 3 shows the relative energy of the bridged form referenced to the gauche structure for each radical. In contrast to the CH_2-$BrCH_2$ and CH_2ICH_2 radicals, the symmetrically bridged conformations of the CF_2XCF_2 radicals are *not* favorable. We could not find any minimum structure with all real frequencies for the symmetrically bridged conformation except for the CF_2-$ClCF_2$ radical calculated at HF level.

Our conclusion that the symmetrically bridged form is not favorable for the CF_2XCF_2 radicals is consistent with recent experimental observations.[11,12] Indeed, the current calculations were motivated by the experiment and the structures and energetics reported herein were used as the initial guess in refining the structure.[11,12] The potential energy surfaces, relevant

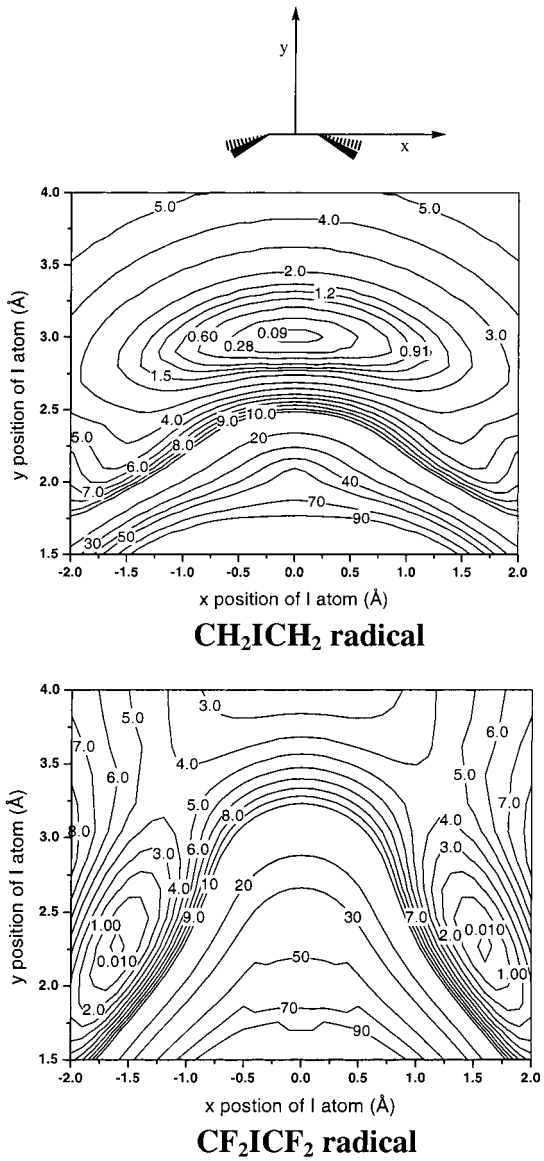

Figure 5. The energy contours for CH_2ICH_2 and CF_2ICF_2 using the B3PW91 (LAV3P) method. The position of halogen atom is referenced to the middle point of two carbon atoms. The zero of energy corresponds to the global minimum. Thus, CH_2ICH_2 is bridged, whereas CF_2ICF_2 has the classical structure.

to the stability of the bridged conformation of CF_2ICF_2 radical, are shown in Figure 5. Using B3PW91, the geometries were optimized as a function of the position of the primary halogen atom. In this calculation, this halogen atom was confined in the XCC plane bisecting the FCF angle. For comparison, the corresponding contour map[1] for the CH_2ICH_2 radical is also presented. The dramatic difference between the CH_2ICH_2 radical and the fluorinated analogue (CF_2ICF_2) is clear. The singly occupied molecular orbital of the bridged structure[1] involves an interaction between the p orbital of halogen atom and the π orbital of the CC bond. The relative instability of the bridged structure in CF_2XCF_2 radicals compared with the CH_2XCH_2 radical is not surprising because the electron density of the π orbital of the C_2F_4 moiety is relatively smaller than that of the C_2H_4 moiety due to presence of highly electronegative F atoms. This was confirmed by calculating the electron density surfaces of C_2H_4 and C_2F_4.

3.3 Dissociation Energy. Using the energies for CF_2XCF_2X and CF_2XCF_2, we calculated the dissociation energy for the reaction of CF_2XCF_2X into CF_2XCF_2 and X. To calculate the

dissociation energy for the further dissociation of CF_2XCF_2 into $CF_2{=}CF_2$ and X, the energy of $CF_2{=}CF_2$ was also calculated at the HF, LMP2//HF, B3PW91 and LMP2 using the 6-31G* basis set. Table 5 lists the calculated dissociation energy for each reaction.

There has been no direct measurement of these dissociation energies. Nathanson, et al.[64] measured the upper limit of 59.1 ± 1 kcal/mol for the reaction enthalpy of CF_2ICF_2I to CF_2CF_2 + I + I using photofragment translational spectroscopy. They also estimated the upper limits to the dissociation energies, CF_2-CF_2−I(Br) → $CF_2{=}CF_2$ + I(Br), of 7.1 ± 2.5 kcal/mol for $D_0(CF_2CF_2{-}I)$ and 22.3 ± 2.5 kcal/mol for $D_0(CF_2CF_2{-}Br)$. We note that these values were obtained by assuming that the C−I bond energies in the CF_2BrCF_2I and CF_2ICF_2I molecules are the same, and equal to $D_0(CF_3CF_2{-}I)$ = 52 ± 1.3 kcal/mol. The dissociation energies for CF_2CF_2−I and CF_2CF_2−Br were also estimated by Krajnovich, et al.[67] using the available thermodynamic data for the related molecules and halogen atoms. They obtained $D_0(CF_2CF_2{-}I)$ of 0 kcal/mol and $D_0(CF_2$-$CF_2{-}Br)$ of 16 kcal/mol by assuming that the C−F bond dissociation energies in CF_2ICF_2 and CF_2BrCF_2 radical are the same as in C_2F_6. They also put an upper limit of $D_0(CF_2CF_2{-}$Br) to 19.3 kcal/mol based on their experimental results.

The values from the B3PW91 (LAV3P(d)) and B3PW91 (MSV(d)) seem to converge to each other and give the best value compared with experiments. The calculated dissociation energies do not contradict these experimental estimates. On the basis of the spread in dissociation energies in Table 5, a conservative estimate for the error bar of the calculations relative to experiment would be 4 kcal/mol. The values calculated at each level of theory follows the same trend; the dissociation energies decrease on the order of Cl, Br, and I. The second dissociation energies (D_2) are much smaller than the first dissociation energies (D_1) mainly due to π-bond formation in $CF_2{=}CF_2$. The C−X bond in the CF_2XCF_2 radical might be weaker than that of CF_2XCF_2X because the hyperconjugative interaction in the radical weakens the C−X bond. As noted before, the C−C bond length of the CF_2XCF_2 radical is considerably shorter and the C−X bond is longer than in the parent molecule. Indeed, $D_1 - D_2 = \pi$, the thermochemical CC π-bond for C_2F_4. Thus, we expect $D_1 - D_2$ to be nearly the same independent of X, which is observed (Table 5).

4.0 Conclusion

The rotational energy barriers of the CF_2XCF_2 radicals (Figures 1, 3) are smaller than those of the parent molecules (CF_2XCF_2X) owing to the absence of steric repulsion between the two heavy halogen atoms. However, the conformational energy differences (Figures 1 and 3) in the radicals were found to be larger than those in the parent molecules. It is suggested that the hyperconjugation between the radical center and the σ^*(C−X) MO stabilizes the anti conformer of the radical.

Compared with haloethyl radicals (CH_2XCH_2), the CF_2XCF_2 radicals show dramatically different behavior. The CF_2XCF_2 radical has two minima and two saddle points, whereas the CH_2-XCH_2 radical has only one minima and one saddle point on the rotational energy surface along the C−C bond. We found that every radical with a $-CH_2$• center has only one stable conformation (anti with one rotational transition structure), whereas radicals with a $-CF_2$• center have two minima and two transition states on the rotational energy surface along the C−C bond. We show that the CF_2XCF_2 radicals cannot form stable bridged structures while such bridged structures *are* favorable in the corresponding CH_2XCH_2 radicals. For the case of X = I, the current calculations were used as the initial guess in refining the structure for a recent ultrafast electron diffraction experiment.[11,12]

TABLE 5: Dissociation Energies from the Optimized Energies Calculated at Various Levels of Theory (HF and B3PW91) and Basis Sets (LAV3P, LAV3P(d), MSV, and MSV(d)) for CF_2XCF_2X and CF_2XCF_2• Radicals (X = I, Br, Cl)

	total dissociation energy		
	$CF_2XCF_2X \rightarrow CF_2CF_2 + X + X$		
method	X = I[a]	X = Br	X = Cl
HF (LAV3P)	11.8	27.5	53.9
HF (LAV3P(d))	21.0	45.2	77.0
LMP2//HF (LAV3P)	46.8	60.0	84.0
LMP2//HF (LAV3P(d))	54.1	76.8	110.7
B3PW91 (LAV3P)	48.0	66.2	91.9
B3PW91 (LAV3P(d))	**55.8**	**80.4**	**110.8**
B3PW91 (MSV)	58.5	74.0	80.6
B3PW91 (MSV(d))	**58.7**	**90.8**	**109.8**
experiment	≤ 59.1 ± 1[b]		
	first dissociation energy (D_1)		
	$CF_2XCF_2X \rightarrow CF_2XCF_2 + X$		
method	X = I[c]	X = Br	X = Cl
HF (LAV3P)	19.8	27.4	40.7
HF (LAV3P(d))	24.3	36.2	52.6
LMP2//HF (LAV3P)	51.4	58.1	70.4
LMP2//HF (LAV3P(d))	46.2	57.4	75.2
B3PW91 (LAV3P)	45.8	55.4	69.3
B3PW91 (LAV3P(d))	**50.4**	**63.4**	**79.8**
B3PW91 (MSV)	51.9	59.7	62.6
B3PW91 (MSV(d))	**50.1**	**67.4**	**77.7**
experiment	52 ± 1.6[d]	67.6 ± 1.6[e]	
	second dissociation energy (D_2)		
	$CF_2XCF_2 \rightarrow CF_2CF_2 + X$		
method	X = I[c]	X = Br	X = Cl
HF (LAV3P)	−8.0	0.1	13.1
HF (LAV3P(d))	−3.1	7.9	24.4
LMP2//HF (LAV3P)	−4.6	−1.1	13.5
LMP2//HF (LAV3P(d))	7.9	19.4	35.5
B3PW91 (LAV3P)	2.2	10.8	22.7
B3PW91 (LAV3P(d))	**5.5**	**17.0**	**31.1**
B3PW91 (MSV)	6.6	14.3	17.9
B3PW91 (MSV(d))	**8.6**	**23.5**	**32.2**
experiment	0[f]	16[f]	
	≤ 7.1 ± 2.5[b]	≤ 22.3 ± 2.5[b]	
	$D_1 - D_2$		
method	X = I[c]	X = Br	X = Cl
HF (LAV3P)	27.8	27.3	27.1
HF (LAV3P(d))	27.4	28.3	28.2
LMP2//HF (LAV3P)	56.0	56.2	56.9
LMP2//HF (LAV3P(d))	38.3	38.0	39.7
B3PW91 (LAV3P)	43.6	44.6	46.6
B3PW91 (LAV3P(d))	**44.9**	**46.4**	**48.7**
B3PW91 (MSV)	45.3	45.4	44.7
B3PW91 (MSV(d))	**41.5**	**43.9**	**45.5**
experiment	~45	~45	~45

[a] The calculated bond energy should be decreased by ~16 kcal/mol to reflect the spin−orbit coupling in the case of X = I. [b] An upper limit obtained by photofragment translational spectroscopy.[64] [c] The calculated bond energy should be decreased by ~8 kcal/mol to reflect the spin−orbit coupling in the case of X = I. [d] $D_0(CF_3CF_2{-}I)$. Direct measured data for $D_0(CF_2ICF_2{-}I)$ is not available.[64] [e] $D_0(CF_3CF_2{-}$Br). Direct measured data for $D_0(CF_2BrCF_2{-}Br)$ is not available.[64] [f] Estimated values by using the available thermodynamic data.[67] [g] Energies are given in kcal/mol. We recommend B3PW91 with a d function (either LAV3P(d) or MSV(d)).

Acknowledgment. This research was funded by a grant (WAG) from the NSF (Grant No. CHE 95-12279) and by contracts (AZ) with the Air Force Office of Scientific Research and the Office of Naval Research. The facilities of the MSC used for these studies are also supported by grants from DOE-ASCI, NSF-MRI, ARO-MURI, Exxon, Chevron Corp., Seiko-Epson, Dow Chemical, Avery Dennison, 3M, the Beckman Institute, Asahi Chemical, and BP Amoco.

Supporting Information Available: Figure S1 showing correlation between the van der Waals radii/group electronegativity and the relative energy difference, and Figures S2-S4 showing the energy decomposition for CH_2ICH_2I, $CF_2ICF_2\bullet$ and $CH_2ICH_2\bullet$, respectively. Table S1 presenting the complete structural parameters of the CF_2XCF_2X and $CF_2XCF_2\bullet$ radicals (X = I, Br and Cl) optimized at various levels of theory (HF and B3PW91) and basis set (LAV3P, LAV3P(d), MSV, MSV-(d)). Table S2 presenting the total energies calculated at various levels of theory and basis set for CF_2XCF_2X and CF_2XCF_2 radicals. Tables S3 and S4 presenting the total energies and relative energies of CH_2XCH_2X calculated at various levels of theory and basis set. Tables S5-S8 presenting the vibrational frequencies and mode analysis for CF_2XCF_2X and CF_2XCF_2 at various levels of theory and basis set. Table S9 listing the exponents and coefficients of MSV(d) basis set. This material is available free of charge via the Internet at http://pubs.acs.org.

References and Notes

(1) Ihee, H.; Zewail, A. H.; Goddard, W. A., III. *J. Phys. Chem. A* **1999**, *103*, 6638.
(2) Kochi, J. K. *Free Radicals*; John Wiley & Sons: New York, 1973; Vol. II.
(3) Beckwith, A. L. J.; Ingold, K. U. *Free-Radical Rearrangements*; Mayo, P. d., Ed.; Academic Press: New York, 1980.
(4) Fossey, J.; Lefort, D.; Sorba, J. *Free Radicals in Organic Chemistry*; John Wiley & Sons: New York, 1995.
(5) Goering, H. L.; Abell, P. I.; Aycock, B. F. *J. Am. Chem. Soc.* **1952**, *74*, 3588.
(6) Thaler, W. *J. Am. Chem. Soc.* **1963**, *85*, 2607−2613.
(7) Skell, P. S.; Tuleen, D. L.; Readio, P. D. *J. Am. Chem. Soc.* **1963**, *85*, 2849.
(8) Tanner, D. D.; Darwish, D.; Mosher, M. W.; Bunce, N. J. *J. Am. Chem. Soc.* **1969**, *91*, 7398.
(9) Skell, P. S.; Shea, K. J. *Bridged Free Radicals*; Kochi, J. K., Ed.; John Wiley & Sons: New York, London, Sydney, Toronto, 1973.
(10) Skell, P. S.; Pavlis, R. P.; Lewis, D. C.; Shea, K. J. *J. Am. Chem. Soc.* **1973**, *95*, 6735.
(11) Cao, J.; Ihee, H.; Zewail, A. H. *Proc. Natl. Acad. Sci. U.S.A.* **1999**, *96*, 338.
(12) Ihee, H.; Lobastov, V. A.; Gomez, U.; Goodson, B. M.; Srinivasan, R.; Ruan, C.-Y.; Zewail, A. H. *Science* **2001**, *291*, 458.
(13) Ihee, H.; Cao, J.; Zewail, A. H. *Chem. Phys. Lett.* **1997**, *281*, 10.
(14) Cao, J.; Ihee, H.; Zewail, A. H. *Chem. Phys. Lett.* **1998**, *290*, 1.
(15) Williamson, J. C.; Cao, J.; Ihee, H.; Frey, H.; Zewail, A. H. *Nature* **1997**, *386*, 159.
(16) Ihee, H.; Cao, J.; Zewail, A. H. *Angew. Chem., Int. Ed.* **2001**, in press.
(17) Koenig, T.; Ball, T.; Snell, W. *J. Am. Chem. Soc.* **1975**, *97*, 662.
(18) Fessenden, R. W.; Schuler, R. H. *J. Chem. Phys.* **1965**, *43*, 2704.
(19) Bernardi, F.; Cherry, W.; Shaik, S.; Epiotis, N. D. *J. Am. Chem. Soc.* **1978**, *100*, 1352.
(20) Goddard, W. A., III; Harding, L. B. *Annu. Rev. Phys. Chem.* **1978**, *29*, 363.
(21) Wiberg, K. B.; Murcko, M. A.; Laidig, K. E.; MacDougall, P. J. *J. Phys. Chem.* **1990**, *94*, 6956.
(22) Engkvist, O.; Karlström, G.; Widmark, P.-O. *Chem. Phys. Lett.* **1997**, *265*, 19.
(23) Thomassen, H.; Samdal, S.; Hedberg, K. *J. Am. Chem. Soc.* **1992**, *114*, 2810.
(24) Iwasaki, M. *Bull. Chem. Soc. Jpn.* **1958**, *31*, 1071.
(25) Glockler, G.; Sage, C. *J. Chem. Phys.* **1941**, *9*, 387.
(26) Simpson, D.; Plyler, E. K. *J. Res. Natl. Bur. Stand.* **1953**, *50*, 223.
(27) Kagarise, R. E. *J. Chem. Phys.* **1957**, *26*, 380.
(28) Kagarise, R. E.; Daasch, L. W. *J. Chem. Phys.* **1955**, *23*, 130.
(29) Serboli, G.; Minasso, B. *Spectrosc. Acta* **1968**, *24A*, 1813.
(30) Thomassen, H.; Hedberg, K. *J. Phys. Chem.* **1992**, *96*, 7983.
(31) Jaguar *Jaguar*; 3.0 ed.; Schrödinger, Inc.: Portland, OR, 1997.
(32) Greeley, B. H.; Russo, T. V.; Mainz, D. T.; Friesner, R. A.; Langlois, J.-M.; Goddard, W. A., I.;; Donnelly, R. E.; Ringnalda, M. N. *J. Chem. Phys.* **1994**, *101*, 4028.
(33) Hay, P. J.; Wadt, W. R. *J. Chem. Phys.* **1985**, *82*, 284.
(34) Exponent, Exponents for d-polarization functions for I, Br, Cl are 0.226, 0.380 and 0.750, respectively.
(35) Rappe, A. K.; Goddard, W. A., III, unpublished results: Exponents and coefficients for C, F, Cl, Br, and I are presented in the Supporting Information.
(36) Becke, A. D. *Phys. Rev. A* **1988**, *38*, 3098.
(37) Slater, J. C. *Quantum Theory of Molecules and Solids*; McGraw-Hill: New York, 1974.
(38) Perdew, J. P.; Chevary, J. A.; Vosko, S. H.; Jackson, K. A.; Pederson, M. R.; Singh, D. J.; Fiolhais, C. *Phys. Rev. B* **1992**, *46*, 6671.
(39) Sæbø, S.; Pulay, P. *Annu. Rev. Phys. Chem.* **1993**, *44*, 213.
(40) Murphy, R. B.; Beachy, M. D.; Friesner, R. A.; Ringnalda, M. N. *J. Chem. Phys.* **1995**, *103*, 1481.
(41) Scott, A. P.; Radom, L. *J. Phys. Chem.* **1996**, *100*, 16 502.
(42) Wong, M. W. *Chem. Phys. Lett.* **1996**, *256*, 391.
(43) Mayo, S. L.; Olafson, B. D.; Goddard, W. A., III *J. Phys. Chem.* **1990**, *94*, 8897.
(44) Phillips, L.; Wray, V. *J. Chem. Soc. Chem. Commun.* **1973**, 90.
(45) Hill, T. L. *J. Chem. Phys.* **1948**, *16*, 399.
(46) Allen, L. C. *Chem. Phys. Lett.* **1968**, *2*, 597.
(47) Lowe, J. P. *Barriers to Internal Rotation about Single Bonds*; Streitwieser, J. A.; Taft, R. W., Eds.; 1968; Vol. 6, pp 1−80.
(48) Abraham, R. J.; Parry, K. *J. Chem. Soc. B* **1970**, 539.
(49) Wolfe, S.; Rauk, A.; Tel, L. M.; Csizmadia, I. G. *J. Chem. Soc. B* **1971**, 136.
(50) Wolfe, S. *Acc. Chem. Res.* **1972**, *5*, 102−111.
(51) Radom, L.; Hehre, W. J.; Pople, J. A. *J. Am. Chem. Soc.* **1972**, *94*, 2371.
(52) Kaloustian, M. K. *J. Chem. Edu.* **1974**, *51*, 777.
(53) Eliel, E. L. *J. Chem. Edu.* **1975**, *52*, 762.
(54) Eliel, E. L.; Juaristi, E. *J. Am. Chem. Soc.* **1978**, *100*, 6114.
(55) Smart, B. E. *J. Org. Chem.* **1973**, *38*, 2039.
(56) Brunck, T. K.; Weinhold, F. *J. Am. Chem. Soc.* **1979**, *101*, 1700.
(57) Kveseth, K. *Acta Chem. Scand. A* **1978**, *32*, 51.
(58) Juaristi, E. *J. Chem. Edu.* **1979**, *56*, 438.
(59) Wiberg, K. B.; Murcko, M. A. *J. Phys. Chem.* **1987**, *91*, 3616.
(60) Dixon, D. A.; Matsuzawa, N.; Walker, S. C. *J. Phys. Chem.* **1992**, *96*, 10 740.
(61) Chang, Y.-P.; Su, T.-M.; Li, T.-W.; Chao, I. *J. Phys. Chem.* **1997**, *101*, 6107.
(62) Bernardi, F.; Bottoni, A.; Fossey, J. *Theo. Chim. Acta* **1982**, *61*, 251.
(63) Knee, J. L.; Khundkar, L. R.; Zewail, A. H. *J. Chem. Phys.* **1985**, *83*, 1996.
(64) Nathanson, G. M.; Minton, T. K.; Shane, S. F.; Lee, Y. T. *J. Chem. Phys.* **1989**, *90*, 6157.
(65) Khundkar, L. R.; Zewail, A. H. *J. Chem. Phys.* **1990**, *92*, 231.
(66) Zhong, D.; Ahmad, S.; Zewail, A. H. *J. Am. Chem. Soc.* **1997**, *119*, 5978.
(67) Krajnovich, D.; Butler, L. J.; Lee, Y. T. *J. Chem. Phys.* **1984**, *81*, 3031.
(68) Engels, B.; Peyerimhoff, S. D. *J. Mol. Struct.* **1986**, *138*, 59.